SEMARAK ILMU PUBLISHING

CFD Letters

Journal homepage:
https://semarakilmu.com.my/journals/index.php/CFD_Letters/index
ISSN: 2180-1363

Variation of Shear Stresses and Flow Dynamics in Stented Patient Specific Carotid Bifurcation Model using Numerical Investigation

Neil Ricardo Almeida[1], Shah Mohammed Abdul Khader[1,*], Hebbandi Ningappa Abhilash[1], Yoshiki Yamaguchi[2], Raghuvir Pai Ballambat[1], Mohammad Zuber[3], Prakashini K[4], Ganesh Kamath S[5], Masaaki Tamagawa[2], Padmakumar R[6], VRK Rao[7], A B V Barboza[1]

[1] Department of Mechanical and Industrial Engineering, Manipal Institute of Technology, Manipal Academy of Higher Education, Manipal – 576104, India
[2] Department of Biological Functions Engineering, Graduate School of Life Sciences and System Engineering, Kyushu Institute of Technology, Kitakyushu, Fukuoka 808-0196, Japan
[3] Department of Aeronautical and Automobile Engineering, Manipal Institute of Technology, Manipal Academy of Higher Education, Manipal-576104, India
[4] Department of Radiology and Imaging, Kasturba Medical College, Manipal Academy of Higher Education, Manipal-576104, India
[5] Department of Cardio-Vascular and Thoracic Surgery, Kasturba Medical College, Manipal Academy of Higher Education, Manipal-576104, India
[6] Department of Cardiology, Kasturba Medical College, Manipal Academy of Higher Education, Manipal-576104, India
[7] Department of Radiodiagnosis, Krishna Institute of Medical Sciences, Secunderabad-500004, India

ARTICLE INFO

Article history:
Received 22 October 2022
Received in revised form 24 November 2022
Accepted 18 December 2022
Available online 1 June 2023

Keywords:
Carotid Stenosis; Carotid Artery Stenting; Pre and post-stenting; Haemodynamics

ABSTRACT

The carotid artery is a clinically important site in the human circulatory system as the consequences of its disease results in adverse outcomes like ischemic strokes, or death for too prolonged ischemia. Understanding the hemodynamics of this artery and its bifurcation are important. A method of treating the stenosis of this artery is Carotid Angioplasty and Stenting (CAS). This procedure results in a heavily modified hemodynamics or state of flow. To understand and predict this flow field modification Computational Fluid Dynamics (CFD) is an important computational tool. Further, the presence of a stent would affect hemodynamics. The aim of this work is to study these effects in patient-specific cases. The reconstructed patient-specific models will form the basis of the construction of the post-stenting carotid bifurcation models. A transient analysis was carried out to estimate the time-varying parameters in the fluid domains over a cardiac cycle as well as to gauge time average values over a cardiac cycle. Results are obtained for hemodynamic parameters, like wall shear stress, velocity, pressure, vorticity, and helicity, in both the prepared stenosed and stented geometries. It is seen that the stenting procedure leads to the renewal of the CCA to ICA flow path. But simultaneously the region in which the stent is present becomes a region of low TAWSS and contains areas of high OSI. These areas of low TAWSS and high OSI within the stented portions of the carotid bifurcations are indications for regions of possible restenosis. Therefore, the investigation demonstrates the likely region for future plaque growth. Further, the effects of widening of the lumen are also noted in comparison to the pre-stent cases.

* *Corresponding author.*
E-mail address: smak.quadri@manipal.edu (Shah Mohammed Abdul Khader)

https://doi.org/10.37934/cfdl.15.6.98114

1. Introduction

The Common Carotid Artery (CCA) is a large elastic blood vessel, and there is one on either side of the body. The left CCA originates from the aorta, which is the largest artery in the human body originating at the heart, whilst the right CCA arises from the brachiocephalic trunk, which itself arises from the aorta. Further each CCA then bifurcates into an Internal Carotid Artery (ICA) and an External Carotid Artery (ECA). The ICA has a larger lumen as compared to the ECA. It must be noted that there is much interindividual variation in the geometry with respect to the precise origin, location and tortuosity of these vessels. There is also much variation within an individual when factors such as posture and body position are considered [1].The carotid artery bifurcation is a site of medical interest due to the severe consequences arising from abnormalities within the vessel wall, namely atherosclerosis, which is essentially the hardening and thickening of the artery wall due to deposits of fat and protein [2]. If the deposit is largely fatty in nature, it is called an atheroma, which is an abnormal lipid mass with a fibrous covering, existing as a discrete, raised plaque under the intima (innermost layer) of an artery. This plaque results in the reduction of flow area in the vessel called a stenosis. The reduced blood flow due to the occlusion leads to further complications like the formation of a thrombus (blood clot) over the plaque or the weakening of the vessel at the site of disease. In either scenario the flow at this site can result in the dislodging of the clot or the plaque, now called an embolus. The embolus can then cause a blockage further downstream. This blockage causes ischemia (insufficient blood flow) in the regions supplied by the artery. In the case where an embolus proceeds along the ICA the region is the brain and this results in a stroke. A stroke, if not fatal, will result in severe brain impairment due to brain tissue death due to a lack of supply of oxygen and nutrients. If the prognosis in the case of a prolonged ischemic stroke is often very poor, and even in cases of a positive outcome, patients, post recovery, tend to experience a lowered quality of life. This is due to the neurological damage that such events lead to.

One of the methods of restoring the lumen of the artery is through carotid angioplasty with stenting as described in Ref. [3]. Stent deployment generally occurs in one of two ways. Either the stent deploys/expands due to its own elasticity and internal restoring forces as seen in the Stryker Wingspan Stent System [4], or the stent is expanded with the help of an angioplasty balloon [5]. Computationally modelling the stent deployment in either case, considering the effects of the elasticity of the diseased blood vessel leads to better preparedness, efficient stent selection and surgery planning, better stent design and better outcomes for patient quality-of-life overall. Carotid artery stenting also comes with the possibility of restenosis, because it gives rise to many pockets of low endothelial shear stress which is a physical manifestation of WSS [6–8] and this is shown to contribute to the change in vascular morphology and eventually restenosis. The nature of the carotid sinus or the carotid bulb as it is also known, is such that it tends to promote flow separation. Sites in the body where such phenomenon occur also tend to be sites of eventual arterial disease. This is no coincidence. The presence of disturbed flow in the carotid bifurcation is an indicator [9, 10]. In the case of an endarterectomy the use of too large a patch closure leads to a large sized sinus, resulting in harmful changes of the hemodynamics [11], possibly leading to deleterious vascular changes.

The hemodynamics (status of blood flow in circulation) of the carotid artery with a stenosis may be evaluated through the use of Computational Fluid Dynamics (CFD). The stent deployment and its interaction with the arterial tissues and plaque materials can be modelled through the use of Finite Element Method techniques. To accurately describe the effects of the dynamic fluid loads of blood on the artery-stent combination, as well as to capture the effects of the elasticity and compliance of the artery-stent combination on the flow of the blood in the vessel a multi-physics approach called Fluid-Structure Interaction is used. Fluid-Structure Interaction is a better approach as it approximates

the fluid and compliant artery to a better extent than just CFD with a rigid artery. As for the model of the carotid artery bifurcation to be used for analysis, the notable ways of obtaining patient-specific geometries are through the reconstructions of data obtained from Magnetic Resonance Angiography (MRA), Magnetic Resonance Imaging (MRI), Computed Tomography (CT) Angiographs, Doppler Ultrasound, etc. Of these CT presents the clearest picture in terms of captured resolution as it is specifically designed to show blood vessels in high contrast. Magnetic Resonance Angiography can also provide relatively high contrast images which are very useful, along with Magnetic Resonance Imaging which uses no additional contrast agents. Doppler Ultrasound is the quickest, cheapest and most widely available method of imaging. In general, Magnetic Resonance Imaging is capable of capturing both the lumen *and* the vessel wall thickness, with its inclusions like plaque, with better detail. Previous works in this area make use of CFD to make predictions about hemodynamic parameters like Wall Shear Stress (WSS) and the Oscillating Shear Index (OSI), both described in chapter 2 of this report, their correlation and how these also correlate to the occurrence of disease in the carotid bifurcation. These use certain parameters and properties to describe the flow of blood in the rigid computational domain. Since, fundamentally, the purely CFD study holds the assumption of a rigid domain wall it is not able to accurately capture the features of the flow and how these features develop over the cardiac cycle in a very accurate way. This is because the compliance of the arterial wall causes significant change in the physical boundary of the computational domain. And this is bound to affect the nature of the flow in the artery. So, although in literature there is an abundance of correlation between modelled hemodynamic flow features, the correlation of hemodynamic parameters and sites of disease, the rigid model cannot be said to be physically accurate.

Arterial wall compliance is also challenging to model due to its inherently anisotropic nature. The mechanical properties of the vessel wall are not the same in the axial and circumferential directions. Not only this but due to the inhomogeneous nature of the arterial wall the stresses vary between the different layers as well [12]. This also poses a challenge when modelling the arterial wall for fluid-structure interaction analysis.

Atherosclerosis has hemodynamic causal factors that have been studied in detail, decades ago by Caro *et al.,* [2]. In addition to forces exerted on the vessel wall, the hemodynamics also accounts for the transport and deposition of nutrients and molecules, like lipids and lipoproteins, in the arterial wall in regions of low and oscillatory wall shear stress (WSS) [7]. For this reason, knowledge of the local hemodynamics in specific regions can help identify sites that are at risk of plaque formation as well as develop a method to predict growth and progression of a plaque [13–15]. The OSI, first described in literature by previous studies [16, 17], is a measure of the porti1on of the cardiac cycle during which a point on the luminal surface experiences a flow that is in a direction other than that of the predominant direction of flow [18]. Bare metal stents have good radial stiffness and prevent serious elastic recoil post-deployment, and therefore reduce the restenosis rate. However, in the later stages of implantation, they will still cause higher rates of in-stent restenosis (ISR) [19].

2. Methodology

2.1 Theory

In a majority of studies blood is treated as a Newtonian fluid, as in Refs. [13, 38, 43, 44]. This is counterintuitive given that blood is known to be a shear thinning non-Newtonian fluid. The primary argument given is the diameter scale for the carotid arteries compared to the constituents that make blood non-Newtonian. And the effect can be neglected due to the high shear rates due to the high velocities [45]. In fact, it does not result in an appreciable effect on the results of the pressure field

according to previous studies [11, 47]. But for stenotic arteries, the effect of blood rheology on the resulting velocity fields and WSS in low-WSS areas is not insignificant [46, 47] and should be considered. liquid. The analysis is carried out by applying Navier-Stokes equations and by using the appropriate viscosity model.

Among the many non-Newtonian models, the Carreau-Yasuda is shown to fit the experimental shear rate relationship well [48]. The Carreau-Yasuda relationship is given by Eq. (1),

$$\frac{\mu - \mu_\infty}{\mu_0 - \mu_\infty} = (1 + (\lambda \cdot \gamma)^a)^{\frac{n-1}{a}} \tag{1}$$

where, μ_0 is the viscosity as zero shear, μ_∞ is the viscosity of the free stream fluid, λ is the relaxation time, γ is the shear rate, n is the power law index and finally a is called the Yasuda exponent.

This relation shows that blood is essentially a shear thinning liquid. This is not an unusual property considering that blood, although appearing to be a continuum of sorts, is actually a multiphase liquid with components like plasma (50-55%), Red blood cells, White blood cells and platelets, with red blood cells being a large portion of the non-plasma component (over 90%) [49].

The number of cardiac cycles executed by the heart or the heart rate is measured in beats per minute (bpm). The heart rate for the average adult is 65 ± 10 bpm [42].

The continuity equation for a fluid the following is obtained as in Eq. (2),

$$\nabla \cdot \vec{U} = 0 \tag{2}$$

further, according to Newton's second law, which is the principle of conservation of momentum which in turn gives the following relation in Eq. (3),

$$\rho \frac{\partial \vec{U}}{\partial t} + \rho(\vec{U} \cdot \nabla)\vec{U} - \nabla \cdot T(\vec{U}) + \nabla p = S \tag{3}$$

where $T(\vec{U}) = \mu(\nabla \vec{U} + \nabla^T \vec{U})$ is the viscous contribution to the Cauchy stress tensor. This equation is the famous Navier-Stokes equation for incompressible flows.

The boundary conditions for a CFD study are also important from the perspective of the correlation of results to real world data.

2.2 Geometry Modelling and Analysis

Computational studies of patient-specific carotid artery bifurcations necessitate the presence of geometric data that may be used to create the fluid and solid computational domains. This is normally obtained by reconstructing the data obtained by Computed Tomography, Magnetic Resonance Imaging or Magnetic Resonance Angiography techniques [1, 9, 17, 20–23] and in some cases Doppler Ultrasound too [32, 40, 41]. The prevalent used of the former group of techniques is due to their superior resolution which then allows for fairly accurate three-dimensional (3D) geometry reconstruction of the required vessel wall (subject to adequate contrast) and the lumen. Although 3D-DUS shows good agreement when lumen cross-sections are concerned, it has limitations like operator dependence and limited field of view, so is not preferred when other sources are available [32]. The fact that reconstructed geometry is representative of the actual arterial geometry *in-vivo* and suitable for numerical studies was demonstrated by Long *et al.,* [23-29], where scans were taken some weeks apart and then the compared based on defined geometric features like the centerline

geometry and lumen area. There was good agreement, showing that the technique of reconstruction based off medical imaging data was suitable for this purpose [27–39].

The patient specific geometries are generated in Mimics Research 21.0 (Materialise, Leuven, Belgium), from Computed Tomography Angiographs. The angiograph 'slices' have a thickness approximately between 0.9mm for the high-resolution studies and 5mm for faster CT studies and pixel dimensions of 0.92mm per pixel dimension. The total resolution in the axial plane was between 356x356 to 512x512 pixels for the patient data. With appropriate thresholding set in Hounsfield Units (HU), the carotid was identified reconstruction was carried out as shown in Figure 1 (a). 3D model obtained after vessel segmentation is as shown in Figure 1(b).

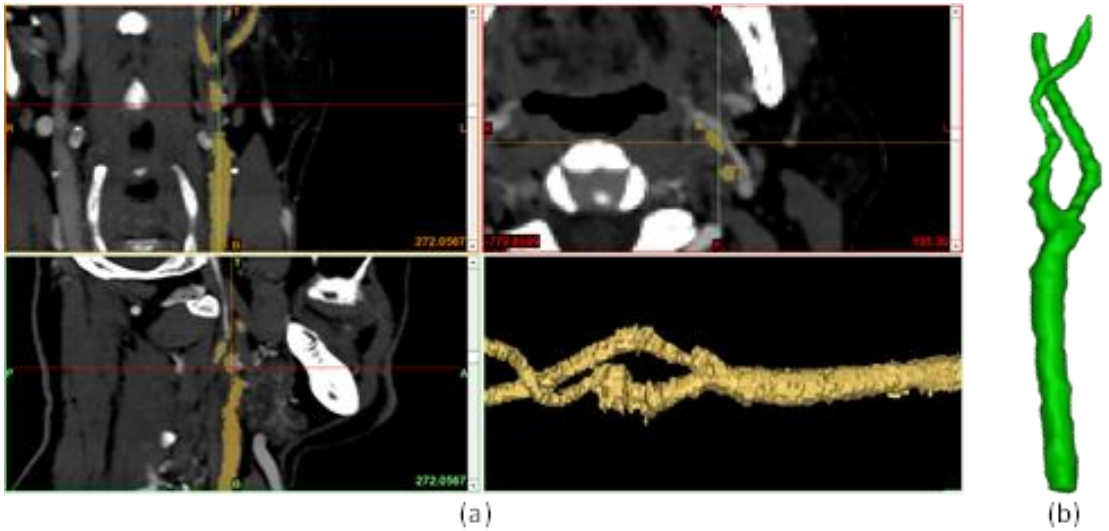

Fig. 1. (a) Patient-specific geometry being segmented and recreated, (b) Geometry of the artery after smoothing the mask

A number of designs of stents are in surgical use for CAS procedures. In order to carry out the placement of the stent in the artery and the creation of the fluid domain post stent placement, the closed-cell stent was modelled based on the commercially available XACT™ Carotid Stent system manufactured by Abbot [50]. It is a closed cell self-expanding nitinol stent. Due to the suggested placement of the stent along the CCA and ICA in the cases considered in this work, a taper stent, model number 82090-01, was selected. This stent has a diameter of 6mm on the distal end and 8mm on the proximal end and is 40mm in length. The stent strut widths and thicknesses were assumed to be 0.12mm, i.e., nearly of a square cross-section. Stent placement in the arteries was carried out by adding the stent to the CAD file, positioning it as recommended by a medical professional and surgeon, and the artery wall was deformed or remodeled to accommodate the stent. A variety of CAD operation were carries out to expand the arterial lumen, place the stent suitably and align it with the centerline of the CCA and so as to manage a physically plausible geometry after placement. The proximal ends of the ICA were moved in space to ensure good alignment prior to lofting and reconstructing cut portions (distal end of ICA). Suitable modifications are made to the files in order to facilitate subsequent geometric operations and avoid errors that may result in zero length geometry and cause bad geometry or CAD operation failures. Having taken care of these issues, the stent is then Boolean subtracted from the modified geometry in order to obtain the fluid region of interest. The total six geometries considered for the analysis is as shown in the Figure 2.

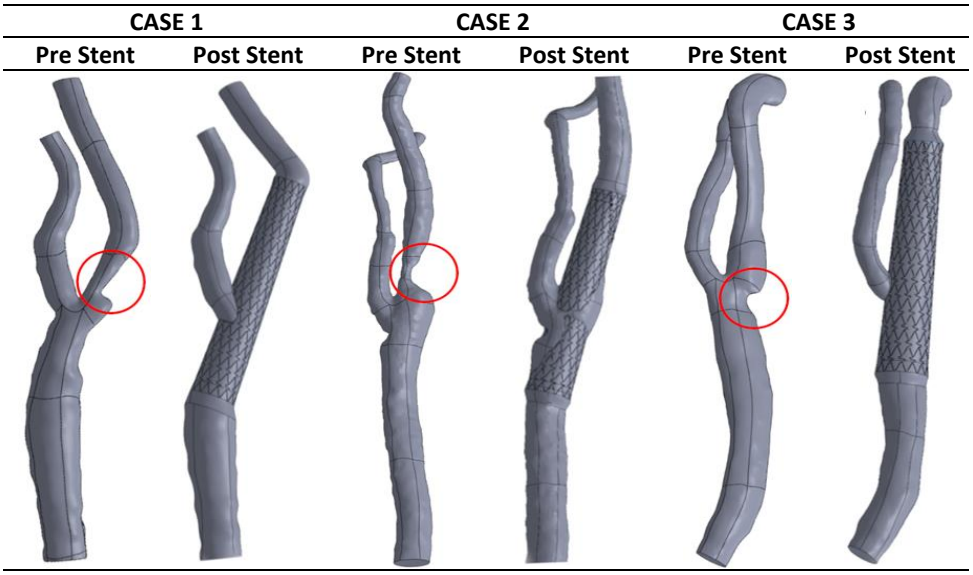

Fig. 2. The pre and post stenting geometries for the three cases with the respective stenosis highlighted.

The CFD analysis is caried out on the prepared fluid domain geometries in ASYS Fluent (Ansys Inc., Canonsburg, PA). The analysis is to be of the transient type since data is to be collected and time averaged over a cardiac cycle. Three cardiac cycles are simulated. This is to ensure any spurious values due to poorly selected initial conditions and assumptions do not carry over into the required period chosen for measurements [third cardiac cycle] and for the transient analysis to stabilise. The time varying velocity profile is specified as an input velocity as shown in Figure 3 (a), for the study by means of a UDF. The time varying pressure profile depicted in Figure 3 (b), is specified as an output over the ICA and ECA ends by means of a UDF. As for the viscosity of blood, the Carreau-Yasuda model is used for analysis and is specified in the same UDF with values of constants picked as per Cho and Kensey [48]. The walls of the fluid domain are a no-slip boundary and this is applied to all walls including the stent's struts. The density of whole blood is taken to be a constant with a value of 1050 $\mathrm{kg/m^3}$. The SIMPLE scheme is adopted for pressure-velocity coupling to enforce mass conservation and to calculate the pressure field. Second order upwind spatial discretisations are used in the solver for accurate results and a higher order term relaxation of 0.4 is specified on the flow variables to avoid the initial instability that arises from using second order upwind schemes with a poor initial guess of the solution. The pressure interpolation scheme is the Standard scheme used by ANSYS Fluent.

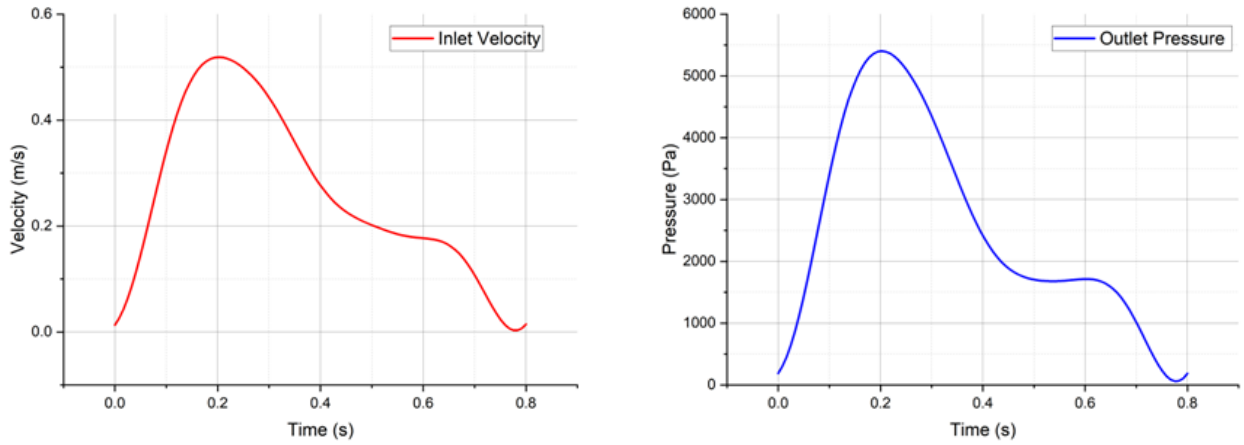

(a) (b)

Fig. 3. (a) The time varying velocity profile, (b) The time varying outlet pressure condition.

3. Results

The results of the CFD studies are presented in this chapter. The results for the stenosed and stented arteries are compared. The differences between the stenosed and stented patient-specific cases are assessed with respect to the region of disease. Further the hemodynamics of the stented arteries are discussed. The results obtained in the third cardiac cycle of the transient CFD analysis at three points in the cycle are presented in the following subsections. They highlight average quantities over the cardiac cycle as well as parameters at specific points in the cardiac cycle which are of interest, namely, early systole, peak systole and early diastole.

3.1 Velocity

In Figure 4, the plots of the velocity streamlines for all three cases are presented, both in the pre and post stenting studies. As expected for the stenosed geometries, the highest velocities in the flow domain occur at or very near the stenosis. This can be explained due to the reduction of flow area due to the reduced lumen size in that region. In all the post stenting cases there is a reduction of the maximum flow velocities in the domain, as expected. The procedure of CAS results in a widened lumen and the reduction of peak velocities seen in the artery is a result of this. Case 1, Case 2 and Case 3 see a reduction of peak velocity of about 34%, 65% and 10%. The drastic reduction in Case 2 is attributed to the severe stenosis. For Case 3, the overall reduction in the peak velocities is not very large. And this is due to the fact that the stenosis for this case was present in the region of the bifurcation and not in the ICA like Case 1 and Case2. The reduction of the arterial lumen was slightly compensated for by the carotid sinus present at the bifurcation.

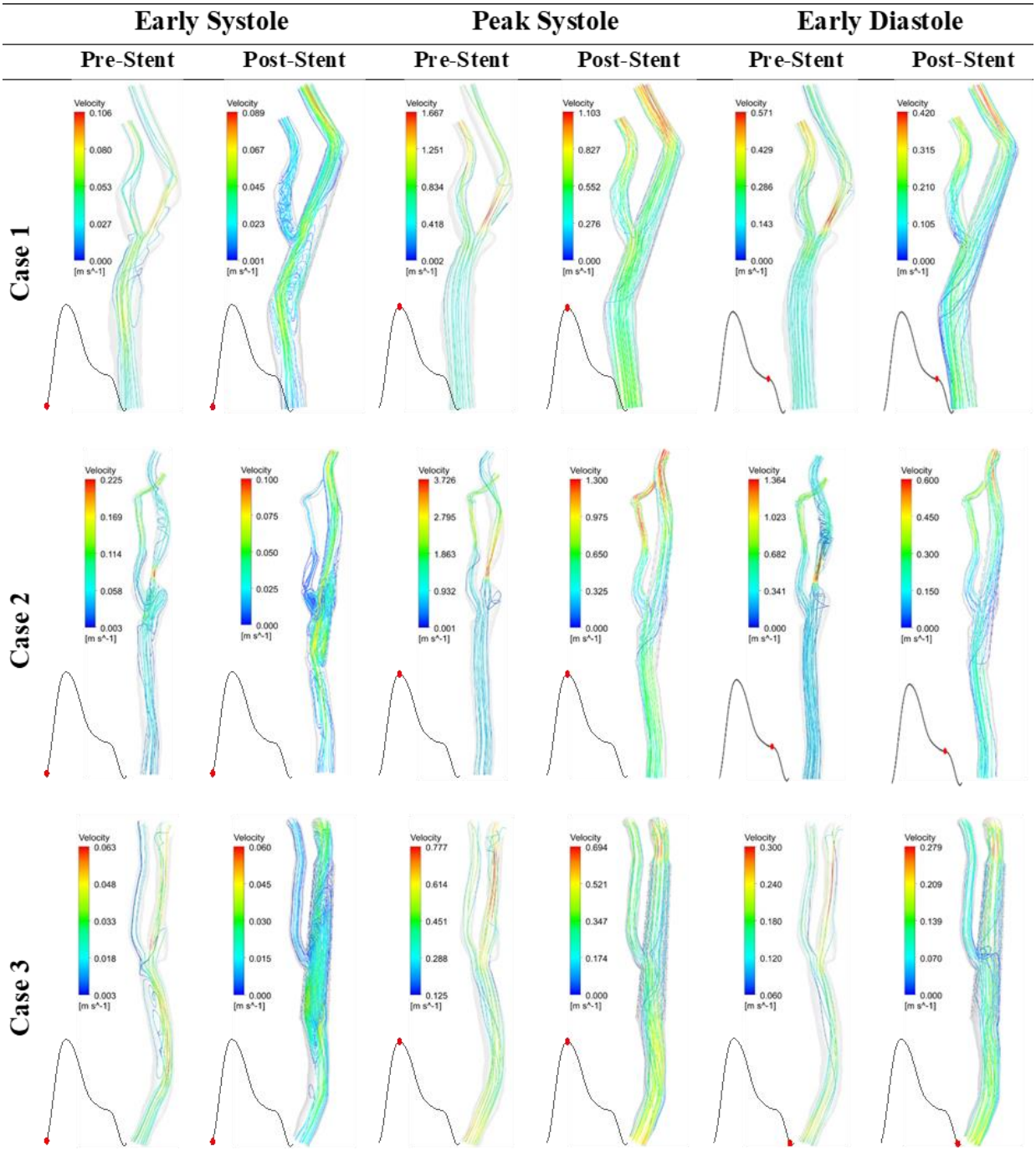

Fig. 4. Velocity streamlines across the three cases, pre and post stenting, compared at 3 points in the cardiac cycle.

3.2 Pressure

In Figure 5 the plots of pressure contours for all three cases are presented, both pre and post stenting. In the pre-stent studies for all patients there is a larger pressure drop between the CCA and the ICA and ECA. The elevated pressures in the CCA region are expected. This would imply that more effort is required to move blood past the stenosis. In the post stenting studies, there is a reduction in pressure drop across the stenosed region across all cases. The stent in the artery removes the restriction caused by the stenosis and so there is less resistance to the flow due to it. Case 1, Case 2 and Case 3 see a reduction of peak CCA pressure of about 13%, 38% and 3%. For Case 2, which has a

particularly severe stenosis, it is evident that the reduction of pressure is significant at peak systole. For Case 3 the overall pressure reduction is not as great as that of the other two cases, and this can be attributed, again, to the fact that the stenosis in this case is located at the bifurcation and not in the CCA itself and because of this the effect of the stenosis is not extremely pronounced.

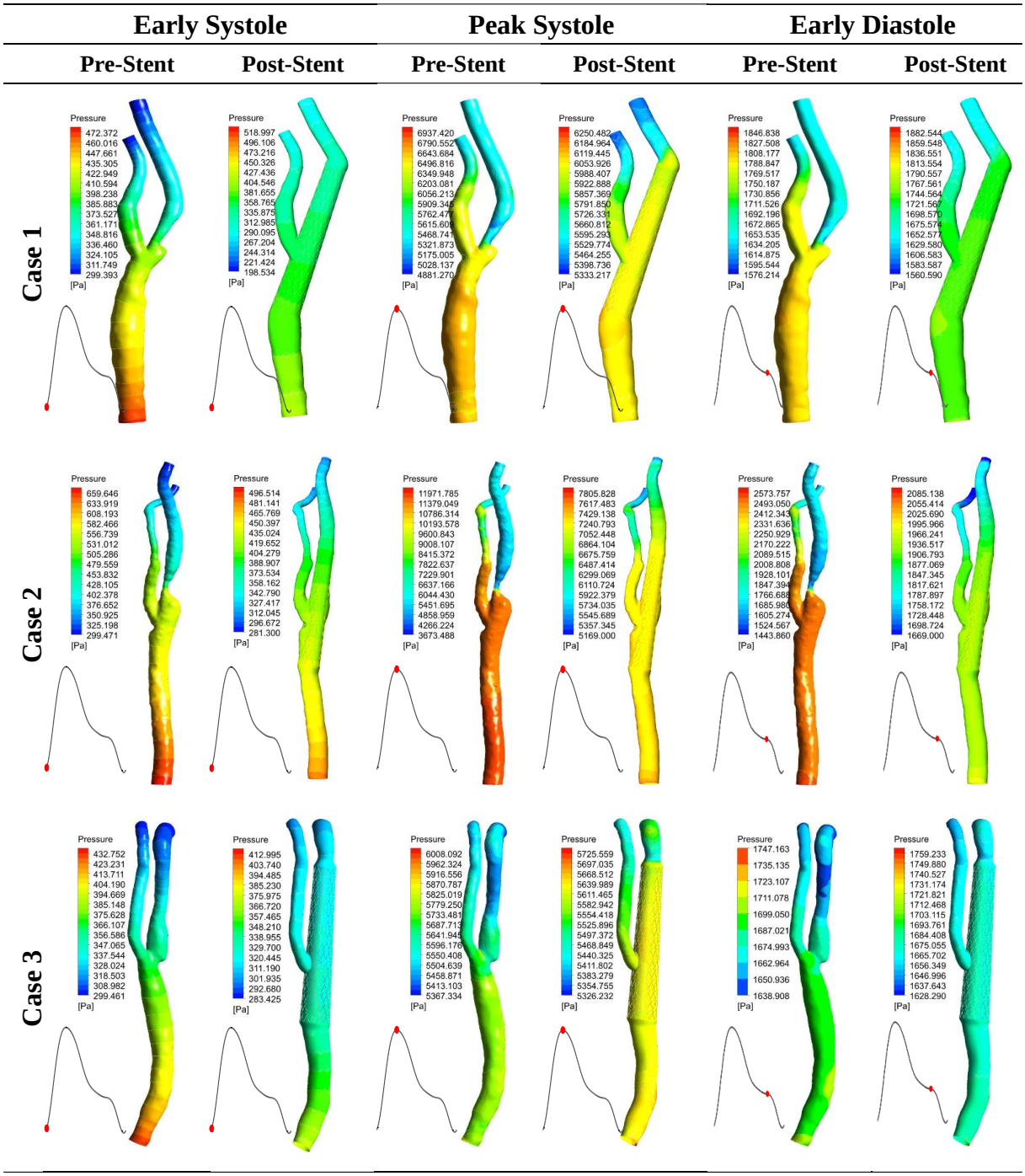

Fig. 5. Plot of pressure contours across the three cases, pre and post stenting, compared at 3 points in the cardiac cycle

3.3 Time Averaged Wall Shear Stress

As seen in Figure 6, for all the pre-stent cases, relatively small regions of low TWSS (shown in red) are observed near the regions of the stenosis. These could contribute to the further growth and

progression of atherosclerotic plaque and is an indicator is plaque growth risk [9]. In the post-stent cases, the observation is that large portions of the stented region experience low TAWSS. This may be associated with the drastic geometric widening in the arterial lumen induced by placement of the stent as well as the presence of the stent itself. The large regions of low TAWSS in the post stenting studies point to increased chances of plaque formation and restenosis. For Case 1, post stenting the low TAWSS area is not as large as that of the other two cases, and this could be explained by the arterial geometry post stenting that causes the incoming flow to impinge upon the arterial wall. This sort of arterial bending when using a stent is seen with more tortuous arterial geometry post stenting when using a closed cell stent.

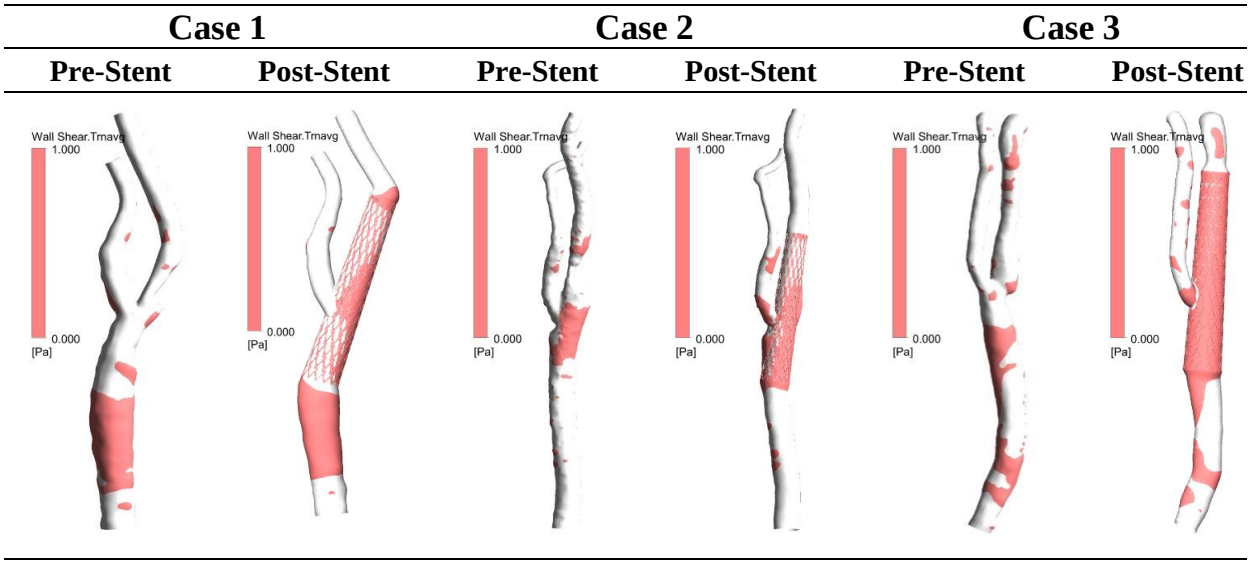

Fig. 6. TAWSS plots for all three cases, pre-stenting and post-stenting

3.4 Vorticity

Vorticity as a quantity mathematically describes the spinning motion or rotation of a parcel of fluid as would be seen by an observer travelling with the fluid parcel in time and space. Figure 7 shows the plots of vorticity for all three cases, both in the pre and post stenting studies. From the figures it is seen that the vorticity, at the beginning and end of the cardiac cycle are relatively low as compared to the vorticity values at peak systole, where the flow velocity is maximum for each respective case.In the stenosed models, very large values of vorticity are seen in the stenosis regions, especially for Case 1 and Case 2. In the case of Case 3, again, since the stenosis is in the bifurcation region, there is a less pronounced increase here. Case 1, Case 2 and Case 3 see a reduction of vorticity at peak systole of about 58%, 60% and 58%. In the post stenting studies, the overall vorticity magnitudes are decreased. The bifurcation apex between the ICA and ECA shows high values of vorticity. But low magnitude vorticity is observed in the stented region likely owing to the discontinuous nature of the artery wall due to the presence of the stent on it. The implication is that the stent leads to some weak near wall vortex generation.

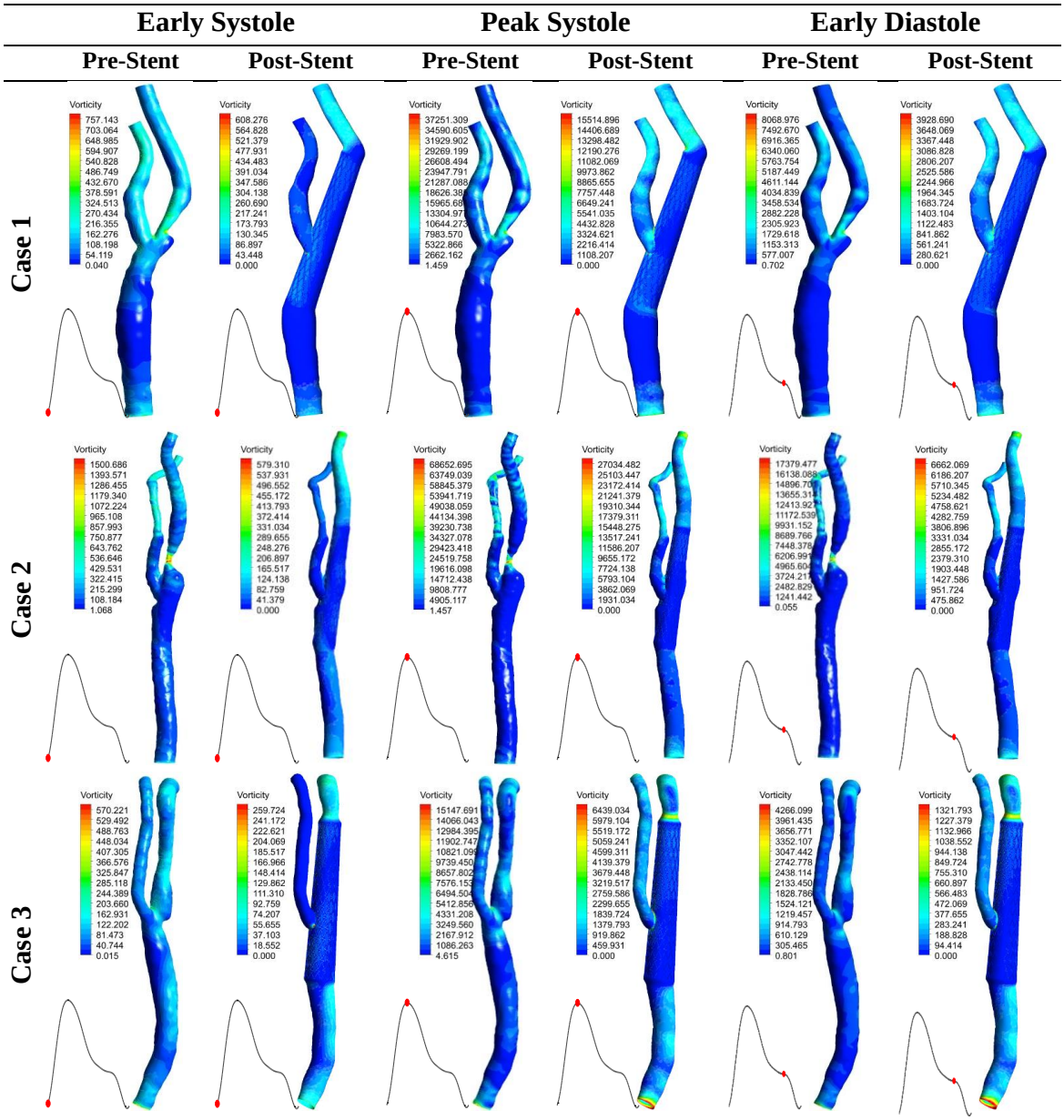

Fig. 7. Vorticity plot for the three cases, pre and post stenting, compared at 3 points in the cardiac cycle

3.5 Oscillatory Shear Index

In Figure 8 the areas of low OSI are shown in white. These regions represent areas on the artery wall that see little to no directional variation of blood flow. The low OSI areas are much larger in the post-stent cases as compared to the stenosed cases. The stents seem to cause a reduction of the locations along which the blood flow oscillates. The presence of the struts of the stent introduces localized zones of high OSI (shown in blue) in the stent region. And this is a factor that may lead to plaque formation and possible restenosis, based on observations made by Lee *et al.,* [9], since these are regions of disturbed flow and also corelate with the areas of low TAWSS. A small amount of flow direction oscillation seems to occur near the stent's struts based on the relatively higher OSI values there, but these regions are not significant in size compared to the neighbouring regions of low OSI.

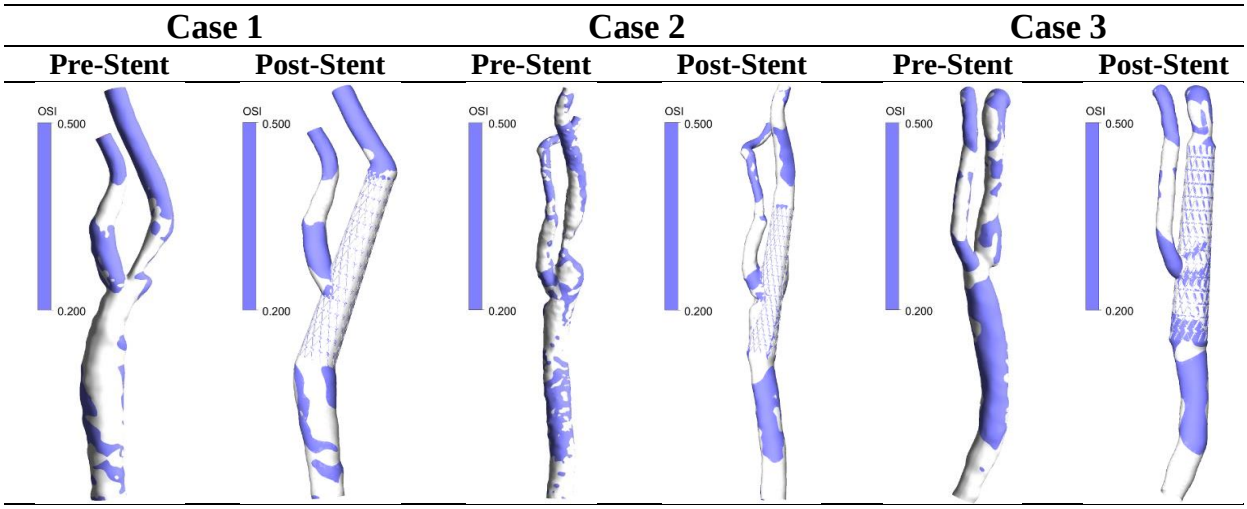

Fig. 8. OSI plots for all three cases, pre-stenting and post-stenting

3.6 Helicity

The helicity plots for all the cases are shown in Figure 9. Helicity is a signed quantity given by the dot product of the velocity vector and the vorticity vector, and tells us about the tendency of the flow to corkscrew along the direction of the flow. A right-handed corkscrew motion is denoted by positive helicity values and left-handed corkscrew motion is denoted by negative values by definition. A general observation is that for all the cases the helicity of the flows appears to reverse at locations where the fluid is redirected rather suddenly. The region of highly helical flow is largest at peak systole in both the pre-stenting and post stenting studies. Largely, the corkscrewing of the flow seems to remain unchanged due to CAS for Case 1 and Case 3 which had a less severe degree of stenosis. For Case 2 the helicity of the flow appears to have changed substantially with the direction of flow rotation seemingly reversed downstream of the stenosis. The struts of the stent also seem to induce vortex formation as mentioned above and this is can be seen in Figure 4 in the post stenting diagrams.

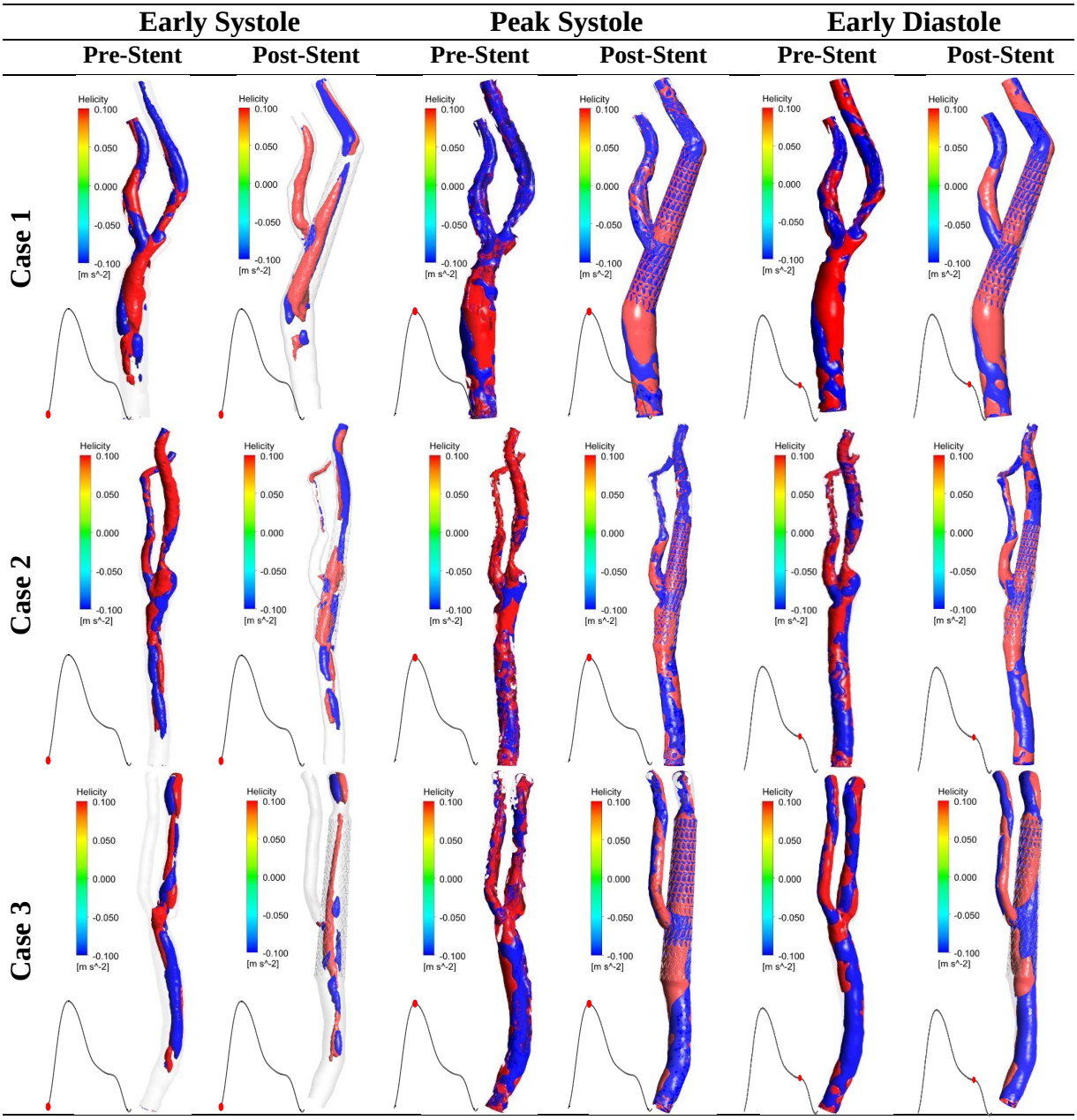

Fig. 9. Helicity plots for the three cases, pre and post stenting, compared at 3 points in the cardiac cycle

4. Conclusions

The goal of this work was to study the variation of shear stresses and hemodynamic parameters in stented patient specific carotid arteries. A comparison of the pre and post stenting geometries is carried out. The reconstructed carotid artery bifurcation geometries were modified to represent the shapes of the patient-specific geometry after a CAS intervention, with the inclusion of the stent. With respect to the TAWSS, it is observed that in the post stenting studies the region in which the stent is deployed corresponds to a region of low average stress. This may be attributed to the marked enlargement that the stent tends to cause in the area in which it is present. This sudden widening results in lower velocities in this region, and hence lower wall shear stresses. When looking at the effects of the stent on the OSI the pre-stenting and post stenting studies, it is apparent that the region of high values of OSI (between 0.2 to 0.5) decrease in the post stenting cases. But regions near the

stent's struts also show up as areas of high values of OSI. As stated in prior literature, areas of low TAWSS and high OSI correlate with location of plaque formation. And from the observations made in this work, there are locations in the stent placement region that fulfill this criterium. This leads us to the conclusion that there exists a possibility that restenosis could occur in the stent containing region. The velocity streamline plots as well as the pressure contours show the remedial effects of CAS. The pressure drops between the CCA and ICA are reduced. And for 2 of 3 cases the rate of flow in the ICA is dramatically restored. Case 1 and Case 2 see an increase of ICA flow velocity, downstream of the prior location of the stenosis, at peak systole of about 90% and 108%. Case 1, Case 2 and Case 3 see a reduction of peak CCA pressure of about 13%, 38% and 3% respectively. The vorticity plots highlight areas where the portions of the flow become rotational. These are areas where flow impingement occurs, like the apex of the carotid bifurcation in both, the pre-stenting and post stenting cases, as well as regions around the stenosis. The helicity plots help visualise the manner in which the arterial blood flow tends to rotate as it flows downstream from the CCA. For the post stenting cases at peak systole, we see that the stent struts, due to their small but definite protrusion from the arterial wall, cause localized pockets of counter rotating fluid spaces.

Acknowledgement
This work is supported by DST-International Bilateral Cooperation Division grant: DST/JSPS/P-293/2019. The authors would like to express their gratitude and sincere appreciation to DST-JSPS for supporting this study.

References

[1] Aristokleous, Nicolas, Ioannis Seimenis, Yannis Papaharilaou, Georgios C. Georgiou, Brigitta C. Brott, Eleni Eracleous, and Andreas S. Anayiotos. "Effect of posture change on the geometric features of the healthy carotid bifurcation." *IEEE transactions on information technology in biomedicine* 15, no. 1 (2010): 148-154. https://doi.org/10.1109/TITB.2010.2091417

[2] Caro, Colin Gerald, Timothy J. Pedley, R. C. Schroter, and WA (eds Seed. *The mechanics of the circulation*. Cambridge University Press, 2012. https://doi.org/10.1017/CBO9781139013406

[3] Townsend, Courtney M., R. Daniel Beauchamp, and B. M. Evers. "Mattox KL Sabiston Textbook of Surgery." (2017): 789-91.

[4] "Wingspan Stent System." Stryker. Accessed November 3, 2021. https://www.stryker.com/ir/en/neurovascular/products/wingspan-stent-system.html

[5] "Deployment Sequence | Tryton Medical - International". Accessed October 30, 2021 https://trytonmedical.com/international/deployment-sequence-2/

[6] Stone, Peter H., Ahmet U. Coskun, Scott Kinlay, Maureen E. Clark, Milan Sonka, Andreas Wahle, Olusegun J. Ilegbusi et al. "Effect of endothelial shear stress on the progression of coronary artery disease, vascular remodeling, and in-stent restenosis in humans: in vivo 6-month follow-up study." *Circulation* 108, no. 4 (2003): 438-444. https://doi.org/10.1161/01.CIR.0000080882.35274.AD

[7] Chatzizisis, Yiannis S., Ahmet Umit Coskun, Michael Jonas, Elazer R. Edelman, Charles L. Feldman, and Peter H. Stone. "Role of endothelial shear stress in the natural history of coronary atherosclerosis and vascular remodeling: molecular, cellular, and vascular behavior." *Journal of the American College of Cardiology* 49, no. 25 (2007): 2379-2393. https://doi.org/10.1016/j.jacc.2007.02.059

[8] Cameron, James N., Ojas H. Mehta, Michael Michail, Jasmine Chan, Stephen J. Nicholls, Martin R. Bennett, and Adam J. Brown. "Exploring the relationship between biomechanical stresses and coronary atherosclerosis." *Atherosclerosis* 302 (2020): 43-51. https://doi.org/10.1016/j.atherosclerosis.2020.04.011

[9] Lee, Sang-Wook, Luca Antiga, J. David Spence, and David A. Steinman. "Geometry of the carotid bifurcation predicts its exposure to disturbed flow." *Stroke* 39, no. 8 (2008): 2341-2347. https://doi.org/10.1161/STROKEAHA.107.510644

[10] Gallo, Diego, David A. Steinman, Payam B. Bijari, and Umberto Morbiducci. "Helical flow in carotid bifurcation as surrogate marker of exposure to disturbed shear." *Journal of biomechanics* 45, no. 14 (2012): 2398-2404. https://doi.org/10.1016/j.jbiomech.2012.07.007

[11] Harrison, Gareth J., Thien V. How, Robert J. Poole, John A. Brennan, Jagjeeth B. Naik, S. Rao Vallabhaneni, and Robert K. Fisher. "Closure technique after carotid endarterectomy influences local hemodynamics." *Journal of Vascular Surgery* 60, no. 2 (2014): 418-427. https://doi.org/10.1016/j.jvs.2014.01.069

[12] Esmaeili Monir, Hamed, Hiroshi Yamada, and Noriyuki Sakata. "Finite element modelling of the common carotid artery in the elderly with physiological intimal thickening using layer-specific stress-released geometries and nonlinear elastic properties." *Computer methods in biomechanics and biomedical engineering* 19, no. 12 (2016): 1286-1296. https://doi.org/10.1080/10255842.2015.1128530

[13] Savabi, Reza, Malikeh Nabaei, Sami Farajollahi, and Nasser Fatouraee. "Fluid structure interaction modeling of aortic arch and carotid bifurcation as the location of baroreceptors." *International Journal of Mechanical Sciences* 165 (2020): 105222. https://doi.org/10.1016/j.ijmecsci.2019.105222

[14] Filipovic, Nenad, Zhongzhao Teng, Milos Radovic, Igor Saveljic, Dimitris Fotiadis, and Oberdan Parodi. "Computer simulation of three-dimensional plaque formation and progression in the carotid artery." *Medical & biological engineering & computing* 51 (2013): 607-616. https://doi.org/10.1007/s11517-012-1031-4

[15] Yang, Chun, Gador Canton, Chun Yuan, Marina Ferguson, Thomas S. Hatsukami, and Dalin Tang. "Advanced human carotid plaque progression correlates positively with flow shear stress using follow-up scan data: an in vivo MRI multi-patient 3D FSI study." *Journal of biomechanics* 43, no. 13 (2010): 2530-2538. https://doi.org/10.1007/s11517-012-1031-4

[16] Algabri, Yousif A., Surapong Chatpun, and Ishkrizat Taib. "An investigation of pulsatile blood flow in an angulated neck of abdominal aortic aneurysm using computational fluid dynamics." *Journal of Advanced Research in Fluid Mechanics and Thermal Sciences* 57, no. 2 (2019): 265-274.

[17] Ku, David N., Don P. Giddens, Christopher K. Zarins, and Seymour Glagov. "Pulsatile flow and atherosclerosis in the human carotid bifurcation. Positive correlation between plaque location and low oscillating shear stress." *Arteriosclerosis: An Official Journal of the American Heart Association, Inc.* 5, no. 3 (1985): 293-302. https://doi.org/10.1161/01.ATV.5.3.293

[18] Azar, Dara, William M. Torres, Lindsey A. Davis, Taylor Shaw, John F. Eberth, Vijaya B. Kolachalama, Susan M. Lessner, and Tarek Shazly. "Geometric determinants of local hemodynamics in severe carotid artery stenosis." *Computers in biology and medicine* 114 (2019): 103436. https://doi.org/10.1016/j.compbiomed.2019.103436

[19] Pan, Chen, Yafeng Han, and Jiping Lu. "Structural design of vascular stents: A review." *Micromachines* 12, no. 7 (2021): 770. https://doi.org/10.3390/mi12070770

[20] Paisal, Muhammad Sufyan Amir, Ishkrizat Taib, Ahmad Mubarak Tajul Arifin, and Nofrizalidris Darlis. "An analysis of blood pressure waveform using windkessel model for normotensive and hypertensive conditions in carotid artery." *Journal of Advanced Research in Fluid Mechanics and Thermal Sciences* 57, no. 1 (2019): 69-85.

[21] Hegde, Pranav, A. B. V. Barboza, SM Abdul Khader, Raghuvir Pai, Masaaki Tamagawa, Ravindra Prabhu, and D. Srikanth Rao. "Numerical Analysis on A Non-Critical Stenosis in Renal Artery." *Journal of Advanced Research in Fluid Mechanics and Thermal Sciences* 88, no. 3 (2021): 31-48. https://doi.org/10.37934/arfmts.88.3.3148

[22] Hegde, Pranav, SM Abdul Khader, Raghuvir Pai, Masaaki Tamagawa, Ravindra Prabhu, Nitesh Kumar, and Kamarul Arifin Ahmad. "CFD Analysis on Effect of Angulation in A Healthy Abdominal Aorta-Renal Artery Junction." *Journal of Advanced Research in Fluid Mechanics and Thermal Sciences* 88, no. 1 (2021): 149-165. https://doi.org/10.37934/arfmts.88.1.149165

[23] Jamali, Muhammad Sabaruddin Ahmad, Zuhaila Ismail, and Norsarahaida Saidina Amin. "Effect of Different Types of Stenosis on Generalized Power Law Model of Blood Flow in a Bifurcated Artery." *Journal of Advanced Research in Fluid Mechanics and Thermal Sciences* 87, no. 3 (2021): 172-183. https://doi.org/10.37934/arfmts.87.3.172183

[24] Ningappa, Abhilash Hebbandi, Suraj Patil, Gowrava Shenoy Belur, Augustine Benjamin Valerian Barboza, Nitesh Kumar, Raghuvir Pai Ballambat, Adi Azriff Basri, Shah Mohammed Abdul Khader, and Masaaki Tamagawa. "Influence of altered pressures on flow dynamics in carotid bifurcation system using numerical methods." *Journal of Advanced Research in Fluid Mechanics and Thermal Sciences* 97, no. 1 (2022): 47-61. https://doi.org/10.37934/arfmts.97.1.4761

[25] Ramdan, Salman Aslam, Mohammad Rasidi Rasani, Thinesh Subramaniam, Ahmad Sobri Muda, Ahmad Fazli Abdul Aziz, Tuan Mohammad Yusoff Shah Tuan Ya, Hazim Moria, Mohd Faizal Mat Tahir, and Mohd Zaki Nuawi. "Blood Flow Acoustics in Carotid Artery." *Journal of Advanced Research in Fluid Mechanics and Thermal Sciences* 94, no. 1 (2022): 28-44. https://doi.org/10.37934/arfmts.94.1.2844

[26] Subramaniam, Thineshwaran, and Mohammad Rasidi Rasani. "Pulsatile CFD Numerical Simulation to investigate the effect of various degree and position of stenosis on carotid artery hemodynamics." *Journal of Advanced Research in Applied Sciences and Engineering Technology* 26, no. 2 (2022): 29-40. https://doi.org/10.37934/araset.26.2.2940

[27] Milner, Jaques S., Jennifer A. Moore, Brian K. Rutt, and David A. Steinman. "Hemodynamics of human carotid artery bifurcations: computational studies with models reconstructed from magnetic resonance imaging of normal subjects." *Journal of vascular surgery* 28, no. 1 (1998): 143-156. https://doi.org/10.1016/S0741-5214(98)70210-1

[28] Botnar, René, Gerhard Rappitsch, Markus Beat Scheidegger, Dieter Liepsch, Karl Perktold, and Peter Boesiger. "Hemodynamics in the carotid artery bifurcation:: a comparison between numerical simulations and in vitro MRI measurements." *Journal of biomechanics* 33, no. 2 (2000): 137-144. https://doi.org/10.1016/S0021-9290(99)00164-5

[29] Long, Q., B. Ariff, S. Z. Zhao, S. A. Thom, A. D. Hughes, and X. Y. Xu. "Reproducibility study of 3D geometrical reconstruction of the human carotid bifurcation from magnetic resonance images." *Magnetic Resonance in Medicine: An Official Journal of the International Society for Magnetic Resonance in Medicine* 49, no. 4 (2003): 665-674. https://doi.org/10.1002/mrm.10401

[30] Marshall, Ian, Shunzhi Zhao, Panorea Papathanasopoulou, Peter Hoskins, and X. Yun Xu. "MRI and CFD studies of pulsatile flow in healthy and stenosed carotid bifurcation models." *Journal of biomechanics* 37, no. 5 (2004): 679-687. https://doi.org/10.1016/j.jbiomech.2003.09.032

[31] Steinman, David A., Jonathan B. Thomas, Hanif M. Ladak, Jaques S. Milner, Brian K. Rutt, and J. David Spence. "Reconstruction of carotid bifurcation hemodynamics and wall thickness using computational fluid dynamics and MRI." *Magnetic Resonance in Medicine: An Official Journal of the International Society for Magnetic Resonance in Medicine* 47, no. 1 (2002): 149-159. https://doi.org/10.1002/mrm.10025

[32] Glor, Fadi P., B. Ariff, L. A. Crowe, A. D. Hughes, P. L. Cheong, SA McG Thom, P. R. Verdonck, David N. Firmin, D. C. Barratt, and X. Y. Xu. "Carotid geometry reconstruction: a comparison between MRI and ultrasound." *Medical physics* 30, no. 12 (2003): 3251-3261. https://doi.org/10.1118/1.1628412

[33] Li, Xiao, Beibei Sun, Huilin Zhao, Xiaoqian Ge, Fuyou Liang, Xuanyu Li, Jianrong Xu, and Xiaosheng Liu. "Retrospective study of hemodynamic changes before and after carotid stenosis formation by vessel surface repairing." *Scientific reports* 8, no. 1 (2018): 5493. https://doi.org/10.1038/s41598-018-23842-0

[34] Wong, Kelvin KL, Pongpat Thavornpattanapong, Sherman CP Cheung, and J. Y. Tu. "Biomechanical investigation of pulsatile flow in a three-dimensional atherosclerotic carotid bifurcation model." *Journal of Mechanics in Medicine and Biology* 13, no. 01 (2013): 1350001. https://doi.org/10.1142/S0219519413500012

[35] Seong, Jaehoon, Woowon Jeong, Nataliya Smith, and Rheal A. Towner. "Hemodynamic effects of long-term morphological changes in the human carotid sinus." *Journal of biomechanics* 48, no. 6 (2015): 956-962. https://doi.org/10.1016/j.jbiomech.2015.02.009

[36] Li, Zhi-Yong, Simon Howarth, Rikin A. Trivedi, Jean M. U-King-Im, Martin J. Graves, Andrew Brown, Liqun Wang, and Jonathan H. Gillard. "Stress analysis of carotid plaque rupture based on in vivo high resolution MRI." *Journal of biomechanics* 39, no. 14 (2006): 2611-2622. https://doi.org/10.1016/j.jbiomech.2005.08.022

[37] Domanin, Maurizio, Diego Gallo, Christian Vergara, Pietro Biondetti, Laura V. Forzenigo, and Umberto Morbiducci. "Prediction of long term restenosis risk after surgery in the carotid bifurcation by hemodynamic and geometric analysis." *Annals of biomedical engineering* 47 (2019): 1129-1140. https://doi.org/10.1007/s10439-019-02201-8

[38] Liu, Xin, Heye Zhang, Lijie Ren, Huahua Xiong, Zhifan Gao, Pengcheng Xu, Wenhua Huang, and Wanqing Wu. "Functional assessment of the stenotic carotid artery by CFD-based pressure gradient evaluation." *American Journal of Physiology-Heart and Circulatory Physiology* 311, no. 3 (2016): H645-H653. https://doi.org/10.1152/ajpheart.00888.2015

[39] Xu, Pengcheng, Xin Liu, Heye Zhang, Dhanjoo Ghista, Dong Zhang, Changzheng Shi, and Wenhua Huang. "Assessment of boundary conditions for CFD simulation in human carotid artery." *Biomechanics and Modeling in Mechanobiology* 17 (2018): 1581-1597. https://doi.org/10.1007/s10237-018-1045-4

[40] Sousa, Luísa C., Catarina F. Castro, Carlos C. António, André Miguel F. Santos, Rosa Maria Dos Santos, Pedro Miguel AC Castro, Elsa Azevedo, and João Manuel RS Tavares. "Toward hemodynamic diagnosis of carotid artery stenosis based on ultrasound image data and computational modeling." *Medical & biological engineering & computing* 52 (2014): 971-983. https://doi.org/10.1007/s11517-014-1197-z

[41] Zain, Norliza Mohd, Zuhaila Ismail, and Peter Johnston. "A Stabilized Finite Element Formulation of Non-Newtonian Fluid Model of Blood Flow in A Bifurcated Channel with Overlapping Stenosis." *Journal of Advanced Research in Fluid Mechanics and Thermal Sciences* 88, no. 1 (2021): 126-139. https://doi.org/10.37934/arfmts.88.1.126139

[42] Hoi, Yiemeng, Bruce A. Wasserman, Yuanyuan J. Xie, Samer S. Najjar, Luigi Ferruci, Edward G. Lakatta, Gary Gerstenblith, and David A. Steinman. "Characterization of volumetric flow rate waveforms at the carotid bifurcations of older adults." *Physiological measurement* 31, no. 3 (2010): 291. https://doi.org/10.1088/0967-3334/31/3/002

[43] Lancellotti, Rocco Michele, Christian Vergara, Lorenzo Valdettaro, Sanjeeb Bose, and Alfio Quarteroni. "Large eddy simulations for blood dynamics in realistic stenotic carotids." *International journal for numerical methods in biomedical engineering* 33, no. 11 (2017): e2868. https://doi.org/10.1002/cnm.2868

[44] Moradicheghamahi, Jafar, Jaber Sadeghiseraji, and Mehdi Jahangiri. "Numerical solution of the Pulsatile, non-Newtonian and turbulent blood flow in a patient specific elastic carotid artery." *International Journal of Mechanical Sciences* 150 (2019): 393-403. https://doi.org/10.1016/j.ijmecsci.2018.10.046

[45] Kumar, Nitesh, SM Abdul Khader, R. Pai, S. H. Khan, and P. A. Kyriacou. "Fluid structure interaction study of stenosed carotid artery considering the effects of blood pressure." *International Journal of Engineering Science* 154 (2020): 103341. https://doi.org/10.1016/j.ijengsci.2020.103341

[46] Guerciotti, Bruno, and Christian Vergara. "Computational comparison between Newtonian and non-Newtonian blood rheologies in stenotic vessels." *Biomedical Technology: Modeling, Experiments and Simulation* (2018): 169-183. https://doi.org/10.1007/978-3-319-59548-1_10

[47] Liu, Haipeng, Linfang Lan, Jill Abrigo, Hing Lung Ip, Yannie Soo, Dingchang Zheng, Ka Sing Wong et al. "Comparison of Newtonian and non-Newtonian fluid models in blood flow simulation in patients with intracranial arterial stenosis." *Frontiers in Physiology* (2021): 1464. https://doi.org/10.3389/fphys.2021.782647

[48] Cho, Young I., and Kenneth R. Kensey. "Effects of the non-Newtonian viscosity of blood on flows in a diseased arterial vessel. Part 1: Steady flows." *Biorheology* 28, no. 3-4 (1991): 241-262. https://doi.org/10.3233/BIR-1991-283-415

[49] "Composition of the Blood | SEER Training". Accessed July 28, 2022 https://www.training.seer.cancer.gov/leukemia/anatomy/composition.html

[50] "Xact Carotid Stent System | Abbott". Accessed March 7, 2022 https://www.cardiovascular.abbott/int/en/hcp/products/peripheral-intervention/carotid-family/xact-carotid-stent-system.html